Engineering Failure Analysis 16 (2009) 1238–1244

Contents lists available at ScienceDirect

Engineering Failure Analysis

journal homepage: www.elsevier.com/locate/engfailanal

Failure analysis of a vibrating shaft in a fretting wear simulator

Young-Ho Lee *, Jae-Yong Kim, Hyung-Kyu Kim

Korea Atomic Energy Research Institute, 150 Dukjin-dong, Yuseong-gu, Daejeon 305-353, Republic of Korea

ARTICLE INFO

Article history:
Received 11 July 2008
Accepted 1 August 2008
Available online 15 August 2008

Keywords:
Failure analysis
Fretting wear simulator
Vibrating shaft
High temperature and high pressure water
Fracture surface

ABSTRACT

Recently, a fretting wear simulator was developed in order to evaluate the fretting wear behavior of nuclear components in high temperature and high pressure (HTHP) water conditions. After 500 h tests, however, two vibrating shafts among four were fractured, which were connected to a specimen holder jig by using a bolt. The fracture surface was examined using both an optical microscope (OM) and a scanning electron microscope (SEM) to determine the failure initiation and failure mode. It was found that the failure had initiated at a contact region between the vibrating shaft and the fuel rod holder jig and a fatigue crack was propagated although it was difficult to prove it conclusively due to the heavily oxidized fracture surface. Near the failure locations, however, the thread hole was subjected to a repeated loading due to the fact that the specimen holder jig had a circular motion for simulating a vibration motion. This suggests that the vibrating shaft failure resulted from corrosion fatigue phenomenon because the fretting test had been performed at high temperature (~320 °C) and pressurized distilled water (~15 MPa) conditions. In this paper, the reasons for this failure and the fracture mechanisms are revealed and discussed by using the OM and SEM results of the failure surface and the stress analysis of the contact regions between the vibrating shaft and the specimen holder jig. Finally, the above results were applied to a design change of the vibrating shaft.

1. Introduction

The failure phenomena of mechanical structures by material degradations in extreme environments have been reported frequently in various industries. One of these examples, is in nuclear power plants (NPPs). Generally, NPPs operate in a high temperature (~320 °C), pressurized water (~15 MPa) and radioactive environment. This condition inevitably results in material degradations such as a corrosion, fatigue, irradiation embrittlement, creep, etc. during their operation. Another severe condition for degrading structural materials is known as a flow-induced vibration (FIV) of relatively slender structures due to the rapid flow velocity of primary and secondary coolants, which results in fretting damages between these slender structures and their supporting structures. These kinds of fretting damages have been experienced in the major components of NPPs such as the nuclear fuel rods, steam generator (SG) tubes and control rods [1]. Among these components, in our laboratory, the fretting wear phenomenon of nuclear fuel rods has been investigated in order to examine and develop a fretting wear mechanism and a defect-free fuel assembly (FA), respectively. Generally, a FA consists of 16×16 or 17×17 nuclear fuel rods, which have the following dimensions; 9.5 mm outer diameter, 0.6 mm wall thickness and about a 4 m length. Because of the FIV phenomenon by a primary coolant, these slender fuel rods could easily vibrate, thus they are supported by several spacer grid structures as shown in Fig. 1. Each cell of a spacer grid structure consists of two springs and four dimples. Therefore, a nuclear fuel rod is supported by a certain amount of spring force, which depends on the spring shape and its stiffness. Under a high temperature in an operating NPP condition, however, the contact force between the fuel

* Corresponding author. Tel.: +82 42 68 8761; fax: +82 42 863 0565.
E-mail address: leeyh@kaeri.re.kr (Y.-H. Lee).

1350-6307/$ - see front matter
doi:10.1016/j.engfailanal.2008.08.013

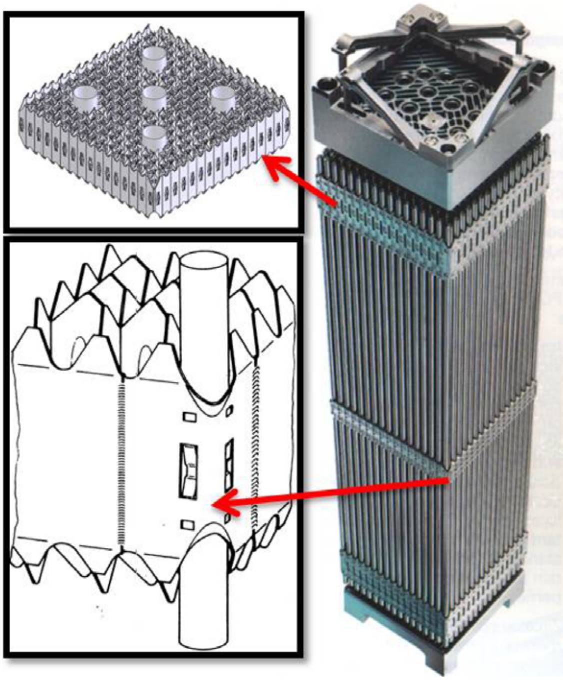

Fig. 1. The schematic view of a nuclear fuel assembly that consists of 16 × 16 or 17 × 17 fuel rods and several spacer grid assembly.

rod and spring/dimple is gradually decreased due to a spring relaxation. In addition, the spring stiffness is also gradually increased because of an irradiation embrittlement of a spacer grid spring/dimple. Even though a certain amount of spring force is exerted on the fuel rod at its initial operation, a relatively small slip amplitude on the contact surface is unavoidable under a severe FIV condition. Consequently, the contact force is gradually decreased and finally, a gap is opened up. This means that the fretting wear mode could be changed from a sliding wear to an impacting wear with increasing operating time. Another important point is that the vibration characteristics of a nuclear fuel rod also changed due to a contact condition change of a fuel rod. Therefore, it is quite difficult to examine the fretting wear mechanism of a nuclear fuel rod in NPP operating conditions.

A vertical type of a fretting wear tester (FRETONUS, FRTtting Tester Of NUclear Systems) for a HTHP water condition was developed in order to evaluate the fretting wear behavior of nuclear components [2]. After 500 h tests, however, two vibrating shafts among four were fractured, which were connected to a specimen holder jig by using a bolt as shown in Fig. 2. It is

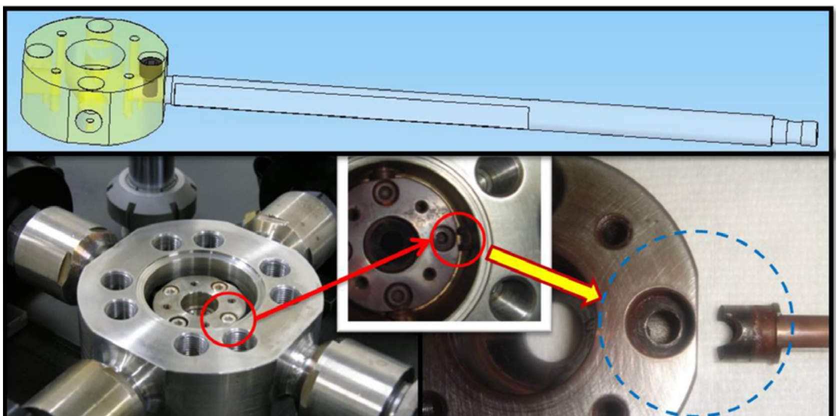

Fig. 2. Schematic views of the assembling method between the vibrating shaft and rod specimen holder jig and the fractured vibrating shaft after 500 h tests at high temperature and pressurized water condition.

essential to evaluate the reason for their failure and to improve the vibrating shaft design to confirm the reliability of the fretting wear tester for a long experiment. In this study, the reasons for the failure and the fracture mechanisms are revealed and discussed by using the OM and SEM results of the fracture surface, measurement of the micro-vickers hardness and the stress analysis of the vibrating shaft. Finally, the above results were applied to a design change of the vibrating shaft.

2. Fracture surface analysis

2.1. OM observation

The vibrating shaft is made of a conventional high-carbon martensitic stainless steel (SUS 440C) and this material is widely used as tools or blades for use in relatively corrosive atmospheres [3]. The chemical composition and mechanical properties are listed in Table. 1. Fig. 3 shows the OM result of the fracture surface for the vibrating shaft. Due to the HTHP water condition, the fracture surface was heavily oxidized and it was difficult to obtain metallographic proof by using the OM observation. However, it is expected that the failure was initiated at a contact region between the vibrating shaft and the fuel rod holder jig because these two parts was assembled by using a bolt as shown in Fig. 2. During the fretting wear tests, four vibrating shafts were reciprocated in their axial direction with a range of ±200 μm, a frequency of 30 °Hz and a sinusoidal motion by two electro-magnetic actuators that were arrayed at an angle of 90°. To generate a circular motion of the fuel rod specimen which is regarded as a conservative simulation of an actual fuel rod vibration in operating NPPs, the phase difference of the sinusoidal waveform for the shake signals of two actuators is set to 90° as shown in Fig. 4. When the fuel rod specimen is vibrated with a circular motion, the contact region of the vibrating shafts with the fuel rod holder jig is expected to experience fatigue loads. Generally, striation traces that are distinct proof for a fatigue failure could be found easily on a fracture surface, if the structural materials are fractured under the fatigue loading conditions. However, the oxidized fracture surface of the vibrating shaft was examined by using SEM without any cleanings because the striation traces could be expected to remove by the oxide removal process (i.e. acid cleaning).

2.2. Hardness variation

Before the SEM observation, it is necessary to examine the mechanical property changes of the vibrating shaft, because it was exposed to the HTHP water condition during 500 h tests. So, a micro-vickers hardness of the fractured vibrating shaft was measured and its result is shown in Fig. 5. It is apparent that the micro-vickers hardness value increased according to the exposed temperature for the vibrating shaft. This result corresponds well with the tempering temperature effect

Table 1
Chemical compositions and mechanical properties (room temperature) of a conventional high-carbon martensitic stainless steel (SUS 440C) [4]

C	Mn	Si	P	S	Cr	Mo	Fe
Chemical compositions (wt%)							
1.0	1.0	1.0	0.04	0.03	17	0.75	Bal.

Yield strength	Tensile strength	Elongation	Elastic modulus	Density	Poisson's ratio
Mechanical properties					
1280 MPa	1750 MPa	4%	200 GPa	7.8 g/cm^3	0.3

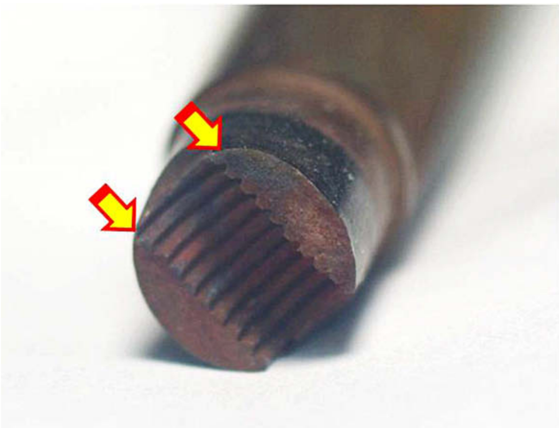

Fig. 3. OM result of the fracture surface for the vibrating shaft: arrows indicate the expected crack initiation region.

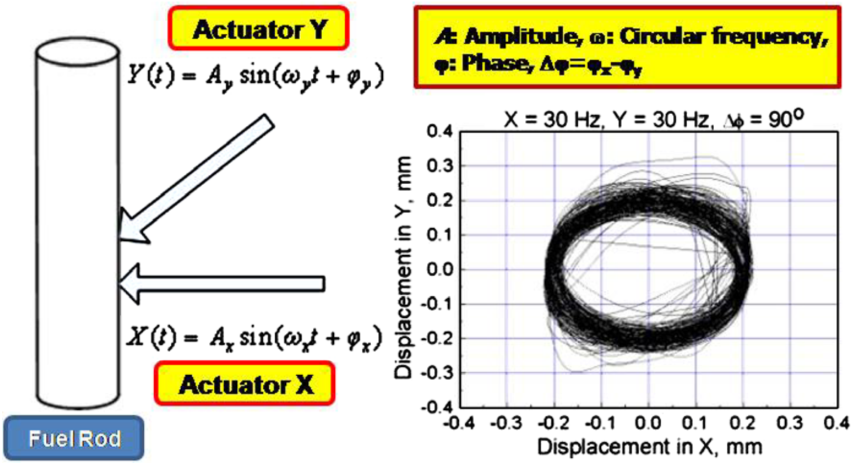

Fig. 4. Actuating mechanism of the fuel rod by using two electro-magnetic actuators in FRETONUS: note that the fuel rod motions are changeable by adjusting vibration amplitudes and phase difference between two actuators.

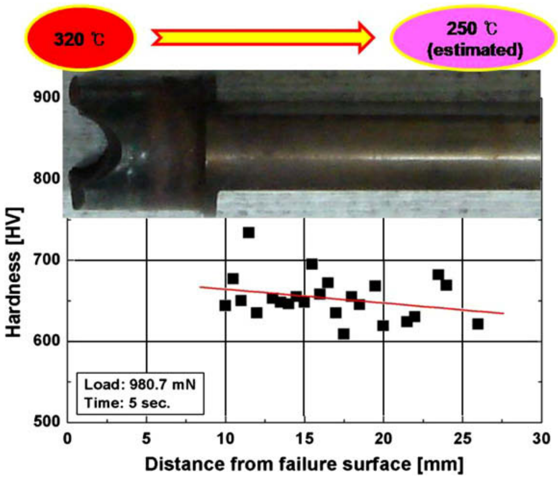

Fig. 5. Measurement result of the micro-vickers hardness according to the exposed temperature for the vibrating shaft.

on the mechanical properties of SUS 440C [4]. In this study, the higher carbon martensitic stainless steel is likely to retain a large amount of untransformed austenite. It is thought that a delayed transformation may occur as temperature fluctuations in several fretting wear tests because the 500 h tests at about 320 °C did not have a negligible effect on the stress relieving of the vibrating shaft material. In addition, it is possible that some loss in ductility may result from a hydrogen embrittlement that is an important concern in martensitic stainless steels in a heat-treating atmosphere containing hydrogen in the form of distilled water.

2.3. SEM results

Fig. 6 shows the morphology of the fracture surface by using SEM. It is apparent that the fracture surface was almost covered with oxides and it is difficult to detect evidence of a fatigue failure such as striation traces. From a careful inspection of the results, however, weak striation traces appeared near a lateral outer surface. Also, a crack propagation trace was found at the contact region between the vibrating shaft and the fuel rod holder jig even though its characteristic could not be defined due to the severe oxidation in the HTHP water condition. One of the interesting results is that an impacting wear scar appeared in the fracture surface of the vibrating shaft. This result means that the impacting wear between the two fractured surfaces is generated after a fracture because the fractured vibrating shaft is continuously reciprocated by an electro-magnetic actuator regardless of the shaft failure. So, it is expected that the fatigue striation traces had disappeared and were covered by the impacting wear motion and by the wear debris with a severe oxidation, respectively. Consequently, the vibrating shaft failure is expected to be initiated by a contact fatigue at the contact region and then the contact force exerted by a bolt

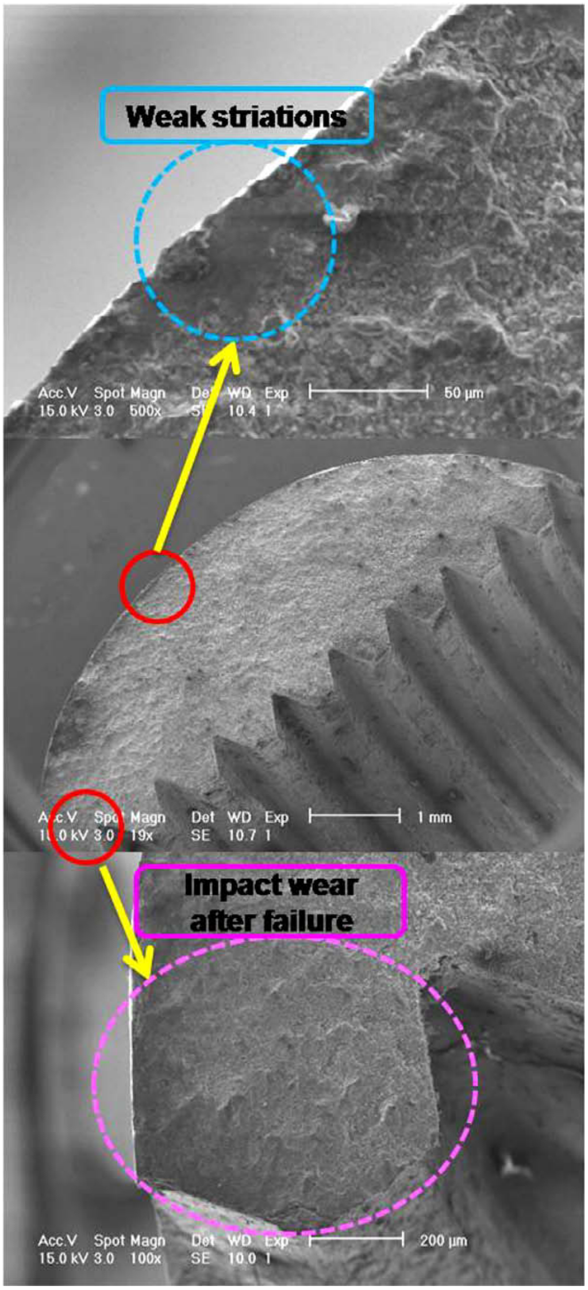

Fig. 6. SEM micrograph of the fractured vibrating shaft surface.

screw will be decreased gradually. At this time, the initial crack propagation is gradually retarded and the contact condition between the vibrating shaft and the fuel rod holder jig will be changed as shown in Fig. 7. So, it is necessary to examine the new crack initiation region by using a stress analysis, which could verify the maximum stress region of the vibrating shaft during a circular motion.

3. Stress analysis

In order to analyze the stress distribution that the vibrating shaft experienced during the initiation of the new crack, the FE model with 10 mm in diameter and 233.5 mm in length was created by using the commercial 3D modeler, SolidEdge V.19 as shown in Fig. 8. The displacement of the constrained cylinder at the left side is 0.2 mm and the connected region with the electro-magnetic actuator at the right side is fixed. The 4 node linear tetrahedron elements were used for the vibrating shaft.

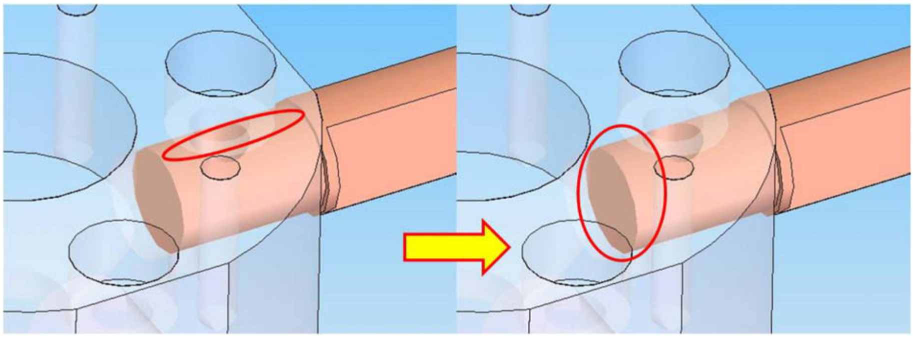

Fig. 7. Variation of contact condition between the vibrating shaft and the fuel rod holder jig after the retardation of initial crack propagation.

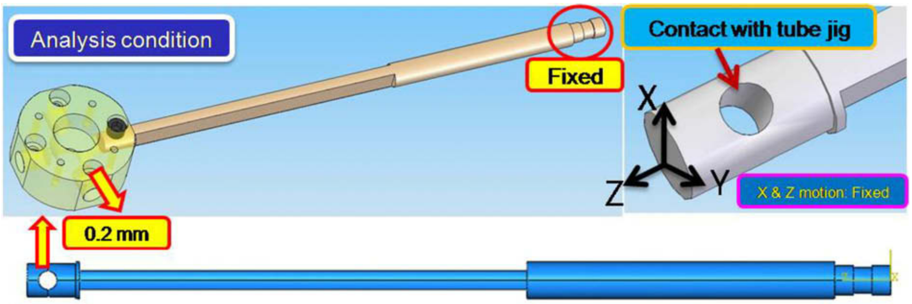

Fig. 8. FE model of the vibrating shaft generated by using a commercial 3D modeler.

The FE model consisted of about 10,100 nodes and 47,200 elements. The used elastic modulus, yield strength, density and Poisson's ratio of the commercial SUS 440C are listed in Table. 1. The commercial code, ABAQUS Standard ver. 6.6–3 [5], was used to post-process the model in order to calculate the Von-Mises stress of the vibrating shaft. The Von-Mises stress dis-

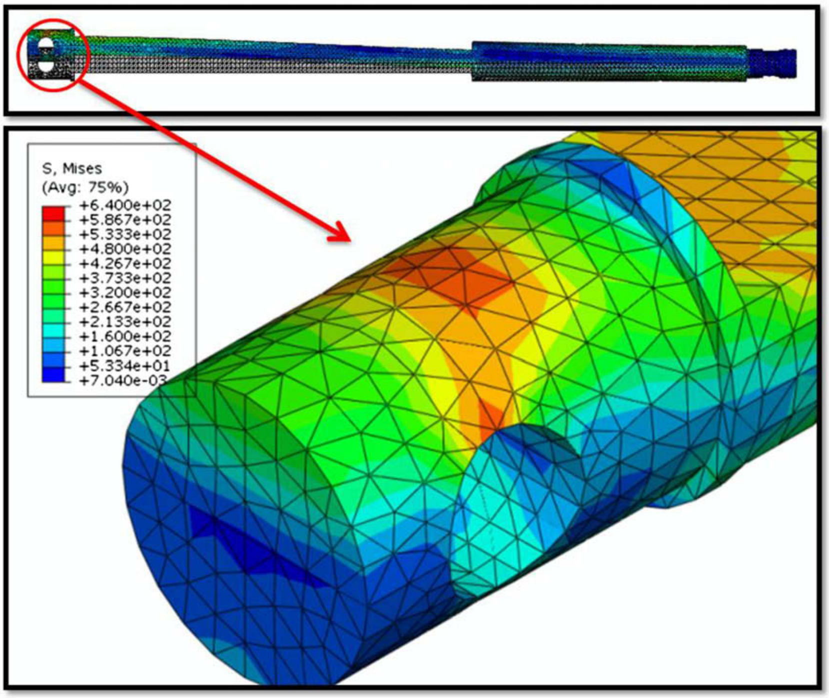

Fig. 9. Model of Von-Mises stress distribution in the vibrating shaft.

tribution in the vibrating shaft showed that the high stress concentrations were present at the edge of the thread hole and the lateral outer surfaces as shown in Fig. 9. In particular, the lateral face experienced stresses in the magnitude of approximately 640 MPa. This value is about half of the yield stress of the vibrating shaft. It is considered that these high stress concentrations are affected by the conservative boundary condition of the FE analysis. Consequently, the positions of the stress concentration are in good accord with the crack generation traces revealed in the SEM observation. Based on this result, the design of the vibrating shaft was modified to reduce the stress concentration between the contact surfaces and the thread hole size of it was decreased to increase the fatigue life cycle.

4. Summary

The reason for the failure of the vibrating shaft in the fretting wear simulator was investigated by using a measurement of the micro-vickers hardness, OM & SEM observations and a finite element analysis. Due to the heavily oxidized fracture surface and the impacting wear between the two fracture surfaces after a failure, it is difficult to obtain the metallographic proof by using the OM observation. However, the failure was expected to initiate at the contact region between the vibrating shaft and the fuel rod holder jig under the fatigue loading conditions. The vibrating shaft failure is expected to be initiated by the contact fatigue at the contact region and then the contact force exerted by a bolt screw will be decreased gradually. After the initial crack propagation is gradually retarded, the change of the contact condition results in a new crack initiation at a lateral outer surface. From the FEA results, the positions of the stress concentrations are in good accord with the crack generation traces revealed in the SEM observation. Based on this result, the design of the vibrating shaft was modified to reduce the stress concentration between the contact surfaces and the thread hole size of it was decreased to increase the fatigue life cycle.

Acknowledgements

This study has been carried out under the Nuclear R&D Program by Ministry of Science and Technology in Korea.

References

[1] Fisher NJ, Weckwerth MK, Grandison DAE, Cotnam BM. Fretting-wear of zirconium alloys. Nucl Eng Des 2002;213:79–90.
[2] Kim HK, Lee YH, Ryew SM, Kim CH, Kim MH. Development of vertical type high temperature and pressure fretting wear tester (FRETONUS). In: Proceedings of KSTLE spring meeting; 2008.
[3] Ojima M, Ohnuma M, Suzuki J, Ueta S, Narita S, Shimizu T, et al. Origin of the enhanced hardness of a tempered high-nitrogen martensitic steel. Scripta Mater 2008;59:313–6.
[4] Davis JR. ASM specialty handbook – stainless steels. ASM International – The Materials Information Society; 1996.
[5] Hibbit HD, Karlsson GI, Sorensen EP. Analysis user's manual (version 6.6). USA; 2006.